Mesenchymal stem cells restore cortical rewiring after neonatal ischemia in mice

Article *in* Annals of Neurology · June 2012

DOI: 10.1002/ana.23543 · Source: PubMed

8 authors, including:

Cindy van Velthoven
Allen Institute for Brain Science
53 PUBLICATIONS **1,682** CITATIONS
SEE PROFILE

Yohan van de Looij
University of Geneva
47 PUBLICATIONS **969** CITATIONS
SEE PROFILE

Annemieke Kavelaars
University of Texas MD Anderson Cancer Center
481 PUBLICATIONS **13,486** CITATIONS
SEE PROFILE

Jitske Zijlstra
University Medical Center Utrecht
19 PUBLICATIONS **764** CITATIONS
SEE PROFILE

Mesenchymal Stem Cells Restore Cortical Rewiring after Neonatal Ischemia in Mice

Cindy T. J. van Velthoven, PhD,[1] Yohan van de Looij, PhD,[2,3] Annemieke Kavelaars, PhD,[1] Jitske Zijlstra, BSc,[1] Frank van Bel, MD, PhD,[4] Petra S. Huppi, MD,[2] Stéphane Sizonenko, MD, PhD,[2] and Cobi J. Heijnen, PhD[1]

Objective: A study was undertaken to investigate the effect of neonatal hypoxic-ischemic (HI) brain damage and mesenchymal stem cell (MSC) treatment on the structure and contralesional connectivity of motor function-related cerebral areas.
Methods: Brain remodeling after HI±MSC treatment in neonatal mice was analyzed using diffusion tensor magnetic resonance imaging, immunohistochemistry, anterograde tracing with biotinylated dextran amine (BDA), and retrograde tracing with fluorescent pseudorabies virus (PRV).
Results: MSC treatment after HI reduced contralesional rewiring taking place after HI. Following MSC treatment, fractional anisotropy values, which were increased in both ipsi- and contralesional cortices and decreased in the corpus callosum (CC) after HI, were normalized to the level observed in sham-operated mice. These results were corroborated by myelin basic protein intensity and staining pattern in these areas. Anterograde tracing of ipsilesional motor neurons showed that after MSC treatment, fewer BDA-positive fibers crossed the CC and extended into the contralesional motor cortex compared to HI mice. This remodeling was functional, because retrograde labeling showed increased connectivity between impaired (left) forepaw and the contralesional (left) motor cortex after HI, whereas MSC treatment reduced this connection and increased the connection between the impaired (left) forepaw and the ipsilesional (right) motor cortex. Finally, the extent of contralesional rewiring measured with BDA and PRV tracing was related to sensorimotor dysfunction.
Interpretation: This is the first study to describe MSC treatment after neonatal HI markedly reducing contralesional axonal remodeling induced by HI brain injury.

ANN NEUROL 2012;71:785–796

Perinatal hypoxia–ischemia (HI) frequently causes encephalopathy associated with cognitive, motor, and behavioral deficits later in life ranging from subtle to severe.[1–3] Although hypothermia improves outcome in term neonates if started within 6 hours after onset of ischemia,[4] there is still an urgent need for effective interventions with an extended therapeutic time window.

Transplantation of mesenchymal stem cells (MSCs) in neonatal and adult animal models of ischemic brain damage promotes functional recovery, associated with neurogenesis, oligodendrogenesis, axonal remodeling, and improvement of motor function.[5–11] The corticospinal tract (CST) represents the primary transmission tract for brain-controlled voluntary movement and consists of axons from pyramidal neurons originating in the motor cortex extending to the contralateral spinal cord.[12] Recently, we showed that MSC treatment following unilateral neonatal HI partially restored the connection between the ipsilesional motor cortex and the contralesional cervical spinal cord, which was disrupted by HI brain damage.[6]

Here, we performed an in-depth analysis of remodeling of motor function-related structures in the brain after MSC treatment following HI. We combined diffusion tensor imaging (DTI) in ipsi- and contralesional motor cortex, corpus callosum (CC), and internal capsule (IC) with immunohistochemical analysis of white matter in these specific brain areas. We also tested the hypothesis

View this article online at wileyonlinelibrary.com. DOI: 10.1002/ana.23543

Received Apr 9, 2011, and in revised form Jan 12, 2012. Accepted for publication Jan 27, 2012.

Address correspondence to Dr Heijnen, Room KC03.068.0, University Medical Center Utrecht, Lundlaan 6, 3584 EA Utrecht, the Netherlands. E-mail: C.Heijnen@umotorcortexutrecht.nl

From the [1]Laboratory of Neuroimmunology and Developmental Origins of Disease, University Medical Center Utrecht, Utrecht, the Netherlands; [2]Division of Child Development and Growth, Department of Pediatrics, University of Geneva, Geneva, Switzerland; [3]Functional and Metabolic Imaging Laboratory, Federal Polytechnic School of Lausanne, Lausanne, Switzerland; and [4]Department of Neonatology, University Medical Center Utrecht, Utrecht, the Netherlands.

that MSC treatment reduces HI-induced rewiring of axons originating from the ipsilesional motor cortex toward the contralesional motor cortex using anterograde tracing of axons from the ipsilesional motor cortex. In addition, we determined to what extent contralesional rewiring represents a functional connection between the contralesional paw and contralesional motor cortex by retrograde labeling of CST motor neurons.

Materials and Methods

MSCs

MSCs isolated from 8-week-old C57Bl/6-Tg(UBC-GFP)30Scha/J-mice (Jackson Laboratories, Bar Harbor, ME) were cultured in MSC expansion medium (Cellular Engineering Technologies, Coralville, IA); MSCs were negative for myeloid and hematopoietic markers and positive for Sca-1, CD90, CD29, CD44, and major histocompatibility complex class I.[7]

Animals

All experiments were approved by the local experimental animal committee. We used the widely used p9 mouse modification described by Hedtjarn et al[13] of the p7 rat Vannucci HI-model, because the p9 mouse brain corresponds developmentally to the term newborn human brain.[14,15] p9 C57Bl/6J-mice underwent right carotid artery occlusion under isoflurane anesthesia followed by 45 minutes of 10% O_2.[13,16] Sham controls underwent anesthesia and incision only. All analyses were performed in a blinded setup.

One hundred thousand MSCs in 2μl phosphate-buffered saline (PBS) or vehicle were infused into the ipsilesional hemisphere at days 3 and 10 after HI.[7]

At 21 days after HI, mice were randomly assigned to tracer injections or magnetic resonance imaging (MRI). Mice assigned to MRI were sacrificed at 28 days after HI; brains were fixed in 4% PFH and stored in PBS until imaging. After imaging, brains were embedded in paraffin. In mice used for MRI, we analyzed DTI data, lesion volume, myelin basic protein (MBP) staining, and motor function.

Mice assigned to tracer injections were injected with 1μl 10% biotinylated dextran amine (BDA; 10,000d; Molecular Probes, Eugene, OR) in PBS at 21 days after HI.[6] At 24 days after HI, 10μl pseudorabies virus (PRV)-614-monomeric red fluorescent protein (mRFP) was injected into the left and PRV-152-enhanced green fluorescence protein (eGFP) into the right forepaw muscle as multiple injections of 1 to 2μl to ensure equal distribution (gifts from Dr L. Enquist). Four days later mice were sacrificed and perfused with 4% PFH, and brains were cryoprotected in 20% sucrose and frozen. In animals used for tracing experiments, we analyzed BDA and PRV labeling, lesion volume, and motor function.

Ex Vivo DTI

MRI analyses were performed using an actively shielded 9.4T/31cm magnet (Varian/Magnex, Palo Alto, CA) with 12cm gradient coils (400mT/m, 120μs) and a transceiver 25mm volume radiofrequency coil. Spin Echo sequence with Stejskal-Tanner diffusion gradients was used.[17] A dual gradient diffusion sampling scheme was used, along 6 opposite directions to cancel b value cross-terms.[18,19] Intensity, duration, and diffusion time were set to 22G/cm, 3 milliseconds, and 19 milliseconds, respectively leading to a b value of 1,185s/mm^{-2}. A field of 15 $\times$ 15mm^2 was sampled on a 128 $\times$ 128 Cartesian grid, given an in-plane pixel size of 117μm, then zero-filled to 256 $\times$ 256. Twelve slices of 0.5mm thickness were acquired in the axial plane. Scans were averaged 12$\times$ with echo time = 35 milliseconds and repetition time = 2,000 milliseconds.

Using Matlab software (Mathworks, Natick, MA), fractional anisotropy (FA) and diffusivity values (mean diffusivity, radial diffusivity [$D_\perp$], axial diffusivity [$D_{//}$]) were derived from the tensor. Regions of interest were delimited on direction-encoded color maps in the CC, cortex, and IC at 6 image planes of the brain from genu to splenium (Fig 1A).

Histology

Serial coronal sections (20μm) were stained with hematoxylin–eosin or mouse anti-MBP (Sternberger Monoclonals, Lutherville, MD) followed by Vectastain ABC kit (Vector Laboratories, Burlingame, CA). PRV was detected using rabbit anti-GFP (GeneTex, Irvine, CA) and biotinylated rabbit anti-RFP (Abcam, Cambridge, MA) followed by donkey antirabbit–AlexaFluor488 and streptavidin–AlexaFluor594 (Invitrogen, Carlsbad, CA). For BDA detection, sections were incubated with streptavidin–AlexaFluor594.

Sections were photographed and analyzed using ImageJ (http://rsb.info.nih.gov/ij/). MBP-positive fiber coherency was quantified using the OrientationJ plugin for ImageJ (http://bigwww.epfl.ch/demo/orientation/) as a measure of (dis)organization. Representative photographs were taken at the same location where cortical DTI analysis was performed (see Fig 1A), and the directionality of fibers was analyzed.

RFP- and GFP-positive cells were counted in the motor cortex, bregma 0.5mm to 2mm. BDA intensity was measured in the CC and contralesional cortex on 6 sequential sections (bregma + 0.55mm) and corrected for BDA intensity at the injection site. BDA labeling at the injection site was confined to a small area and not significantly different between groups (raw BDA intensity at injection site: sham, 270,519 $\pm$ 59,471 absorbance units [AU]; HI, 305,821 $\pm$ 110,150AU; HI + MSC, 270,458 $\pm$ 95,825AU, $p = 0.97$).

Motor Function

Cylinder rearing test was used to assess forepaw preference in both mice sent for DTI analysis and mice used for tracer experiments. Weight-bearing forepaws contacting the wall during full rear were recorded. Nonimpaired forepaw preference was calculated as ([nonimpaired $-$ impaired]/[nonimpaired + impaired + both forepaws]) $\times$ 100%.[7,16]

Statistical Analysis

Data represent means $\pm$ standard error of the mean. MRI data were analyzed by Mann–Whitney, histology measures using

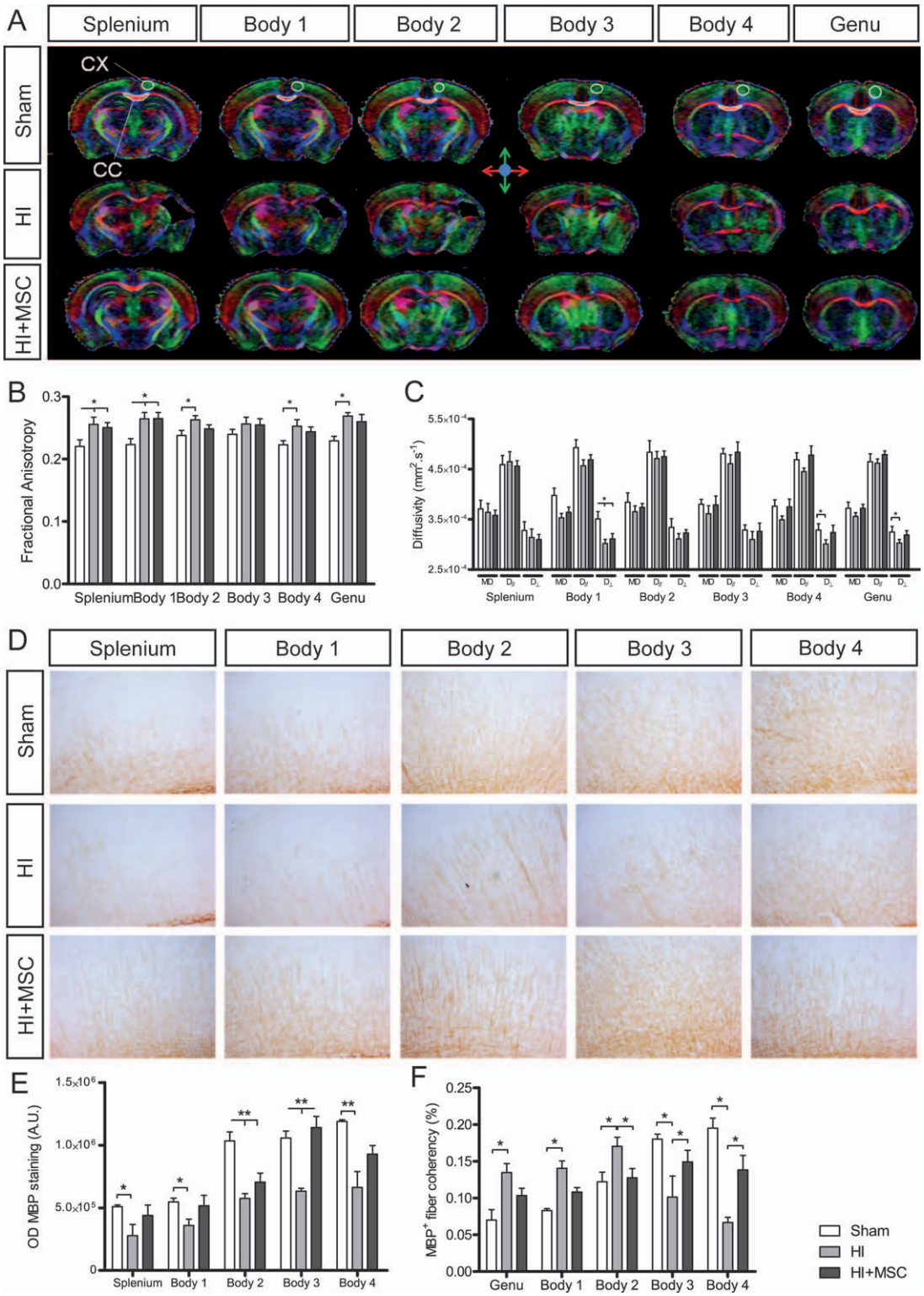

FIGURE 1: Structural changes in the ipsilesional cortex after hypoxia–ischemia (HI) and mesenchymal stem cell (MSC) treatment. (A) Direction-encoded color maps are shown of a typical brain from the sham, HI, and HI + MSC groups at 6 different image planes from the genu to the splenium of the corpus callosum. Histograms of the (B) fractional anisotropy and (C) diffusivity values measured in the ipsilesional cortex are shown. (D) Representative photographs of myelin basic protein (MBP) staining in the cortex are shown. (E) MBP staining intensity and (F) fiber coherency as a measure of (dis)organization of MPB-positive fibers were measured in the cortex. MBP staining and analysis were performed in mice assigned to magnetic resonance imaging. Data are expressed as mean ± standard error of the mean, *$p < 0.05$, **$p < 0.01$; n = 8 mice per group. AU = absorbance units; $D_\perp$ = radial diffusivity; $D_{//}$ = axial diffusivity.

1-way analysis of variance (ANOVA) with Bonferroni post-tests, and behavior using 2-way ANOVA with Fisher least significant difference post-tests. Pearson test was used for correlation analysis; $p < 0.05$ was considered statistically significant.

Results

Anatomical Changes after HI and MSC Treatment

On MRI, several mice in the HI group displayed a clear anatomical dissymmetry on T2-weighted (T2W) images (Fig 2A). After MSC treatment, fewer anatomical abnormalities were observed. T2W images indicated that MSC treatment significantly reduced HI-induced loss of ipsilesional hemispheric volume (see Fig 2B, C).

At the functional level, MSC treatment after HI significantly increased sensorimotor function as measured at 21 and 28 days after the insult (see Fig 2D).

Changes in the Ipsilesional Cortex after HI and MSC Treatment

DTI was used to further examine effects of MSC treatment following HI on brain microstructure. In the ipsilesional motor cortex, MSC treatment decreased FA values at levels body4 and genu to the levels seen in sham-operated animals (see Fig 1B), whereas following HI FA values increased at all levels except body3.

MSC treatment normalized $D_{\perp}$ in body4 and genu of the motor cortex, which was decreased after HI, to the level seen in sham-operated mice (see Fig 1C). These results encouraged us to examine myelination in the motor cortex of the same mice in more detail. In the ipsilesional cortex, MSC treatment increased MBP intensity at levels body3 and body4 when compared to HI mice (see Fig 1D, E). Furthermore, this increase in MBP intensity after MSC treatment reached the intensity observed in sham-operated mice at all levels except body2. In the ipsilesional cortex, HI decreased MBP intensity at all levels.

MBP-positive fiber coherency was significantly increased at some regions of the CC (body3 and body4), but in other regions the opposite trend was observed (body2) when compared to HI. The overall return to the level seen in sham-operated mice after MSC treatment indicates restoration of fiber alignment (see Fig 1D, F). MBP-positive fiber coherency was quantified as a measure of (dis)organization in the ipsilesional cortex. Following MSC treatment, MBP-positive pattern at levels splenium, body1, and body2 appeared as fibers with many lateral arborizations, as also seen in sham-operated mice. In contrast, HI induced a more linear MBP-positive pattern with fewer lateral arborizations, which coincides with a higher fiber coherency, than in sham or MSC-treated mice.

Connectivity between Ipsilesional and Contralesional Cortices

Next, we established whether changed organization in the ipsilesional cortex as detected by DTI and MBP analysis was associated with rerouting of axons originating from the ipsilesional motor cortex. In the CC, FA values decreased following HI and were normalized by MSC treatment at all levels except body4 (Fig 3A). Callosal DTI measures were equal between sham and MSC-treated mice on all image planes (see Fig 3B). In contrast, following HI, $D_{//}$ decreased at all image planes except genu, indicating changes in CC microstructure. At the microscopic level, MSC treatment increased MBP intensity at levels body2 and body3 when compared to HI mice and did not differ from sham-operated mice (see Fig 3C, D).

Subsequently, we injected BDA into the ipsilesional motor cortex in a separate group of mice. BDA is taken up mostly by somata of neurons and transported anterogradely to axon terminals, allowing detailed analysis of axons originating from the ipsilesional motor cortex.[20]

In sham-operated mice, very few BDA-positive fibers cross the CC (Fig 4A), and as a result BDA intensity in the contralesional cortex was low (see Fig 4B). MSC treatment significantly decreased the number of HI-induced fibers crossing the CC toward the contralesional hemisphere. Concomitantly, BDA intensity in the contralesional motor cortex following MSC treatment is lower when compared to HI.

Following MSC treatment, contralesional cortex changes were also detected by DTI, as FA values were decreased at level body4 and genu when compared to HI (see Fig 4C). Figure 4D depicts a schematic representation of BDA-labeled axons in the sham brain and after HI and MSC treatment.

Functional Connections between Contralesional Motor Cortex and HI-Impaired Forepaw

Our next question was whether this contralesional rewiring affected ipsilesional routing of the CST. Motor axons form a tract running from the ipsilesional cortex, passing the ipsilesional IC toward the contralesional spinal cord. DTI analysis of the IC revealed that MSC treatment increased FA in both ipsi- and contralesional IC when comparing HI mice to FA observed in sham-operated mice (Fig 5A). These results indicate that MSC treatment reduces the extensive HI-induced contralesional axonal rewiring. Therefore, we hypothesized that axons crossing the CC are functionally connected to the

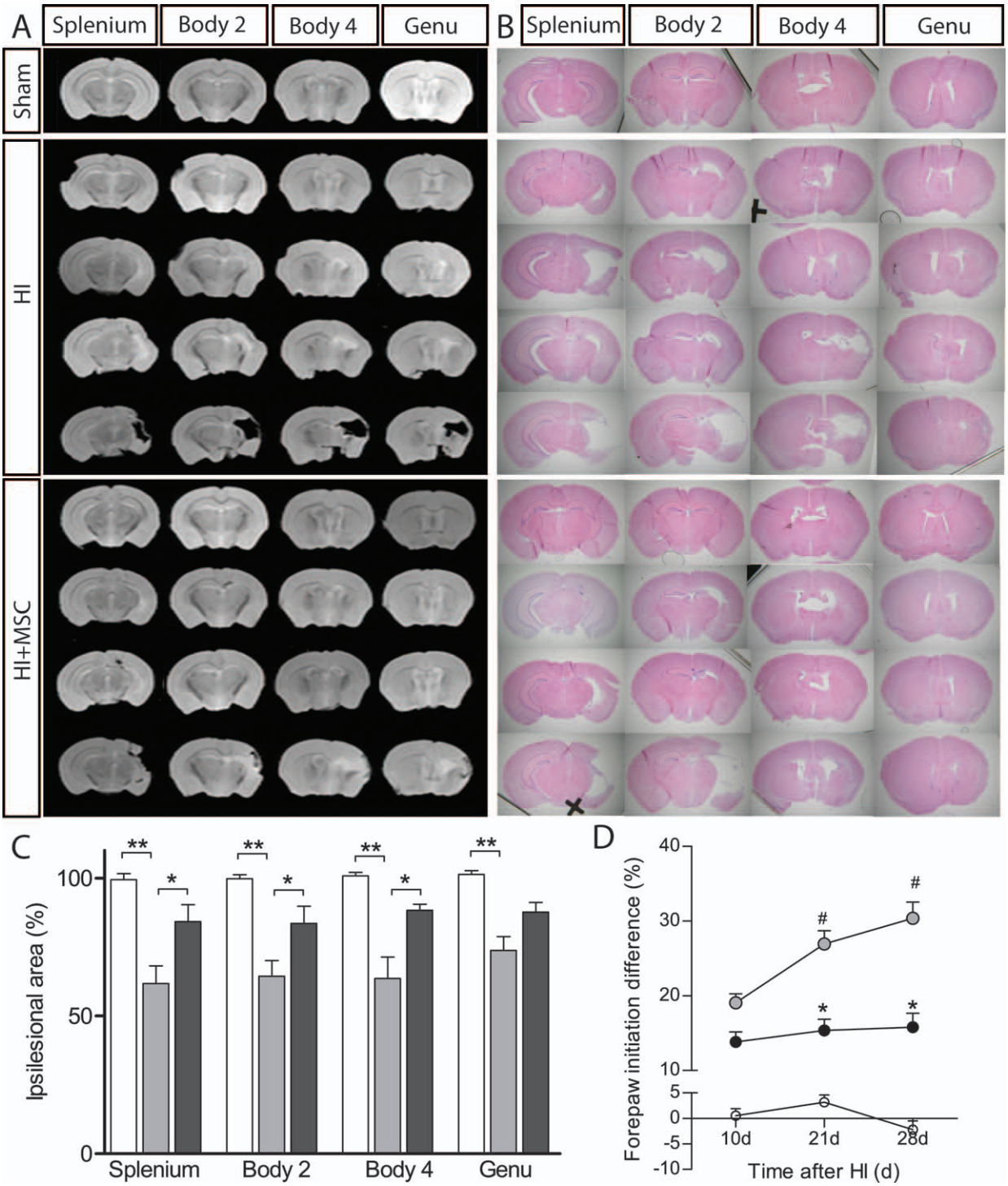

FIGURE 2: Anatomic changes in the brain after hypoxia–ischemia (HI) and mesenchymal stem cell (MSC) treatment. Mice were exposed to HI at p9 and received MSCs (HI + MSC) or vehicle (HI) at 3 and 10 days after HI. (A) Paraformaldehyde-fixed brains obtained at 28 days after HI were scanned by magnetic resonance imaging (MRI) ex vivo, and T2-weighted (T2W) images are presented to visualize anatomical damage. T2W images were confirmed by histological analysis of brain damage. (B) Brains of mice assigned to MRI analysis and tracer injections were stained with hematoxylin–eosin, and (C) ipsilesional area was determined. Sham *(white bars)*, n = 12; HI *(light gray bars)*, n = 19; HI + MSC *(dark gray bars)*, n = 19. Data represent mean ± standard error of the mean (SEM), *$p < 0.05$, **$p < 0.01$. (D) Preference to use the nonimpaired paw in the cylinder rearing test was determined at 10, 21, and 28 days after HI in mice assigned to MRI and tracer injections, and data were analyzed using 2-way analysis of variance with factors time and treatment taken into consideration. Sham *(white dots)*, n = 12; HI *(light gray dots)*, n = 19; HI + MSC *(dark gray dots)*, n = 19. Data represent mean ± SEM, $^{\#}p < 0.01$ versus HI at 10 days; *$p < 0.01$ versus vehicle at the same time point.

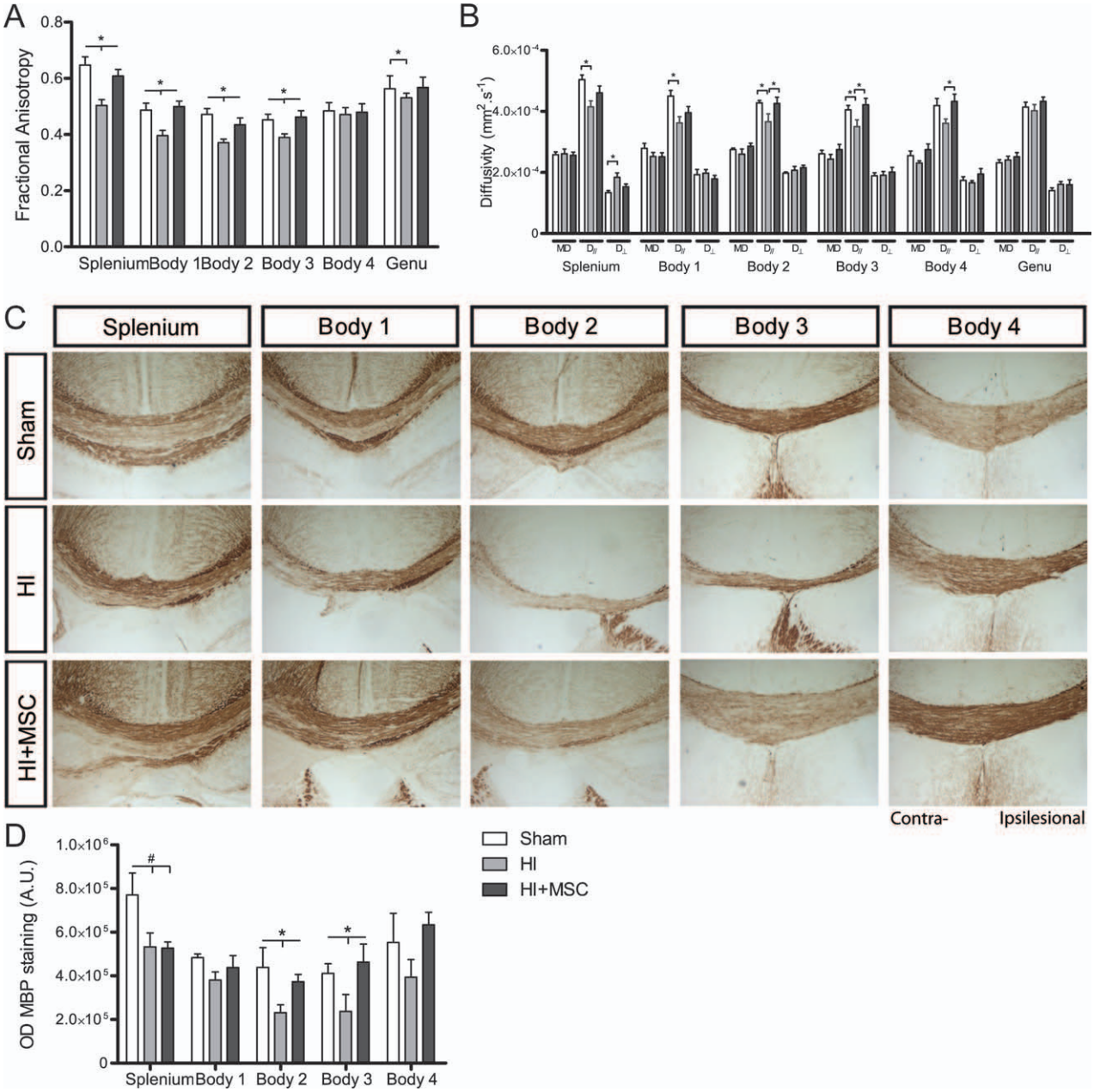

FIGURE 3: Structural changes in the corpus callosum after hypoxia–ischemia (HI) and mesenchymal stem cell (MSC) treatment. In the corpus callosum, changes in (A) fractional anisotropy and (B) diffusivity were analyzed after HI and MSC treatment. (C) Representative photographs of the corpus callosum stained for myelin basic protein (MBP) correspond to the 5 image planes from splenium to body4, and (D) MBP intensity was measured at those locations. MBP staining and analysis were performed in mice assigned to MRI. Data are expressed as mean ± SEM. $^{\#}p < 0.05$ versus sham, $^{*}p < 0.05$ versus HI; n = 8 mice per group. AU = absorbance units; $D_{\perp}$ = radial diffusivity; $D_{//}$ = axial diffusivity.

contralesional cortex to control the impaired forepaw. This hypothesis was tested using the retrograde trans-synaptic PRV-614-mRFP and PRV-152-eGFP tracers in a separate group of mice.[21,22]

PRV-614-mRFP was injected into the (HI-impaired) left forepaw (see Fig 5B). As anticipated, in sham-operated mice, clear mRFP-positive neurons were visible in the right motor cortex, with hardly any mRFP-positive neurons in the left motor cortex (see Fig 5C, D). However, after HI only few mRFP-positive neurons were visible in the ipsilesional (right) motor cortex, whereas the number of mRFP-positive neurons in the contralesional (left) motor cortex was increased. Importantly, after MSC treatment of HI mice, mRFP labeling partially returned to the pattern observed in sham-operated mice.

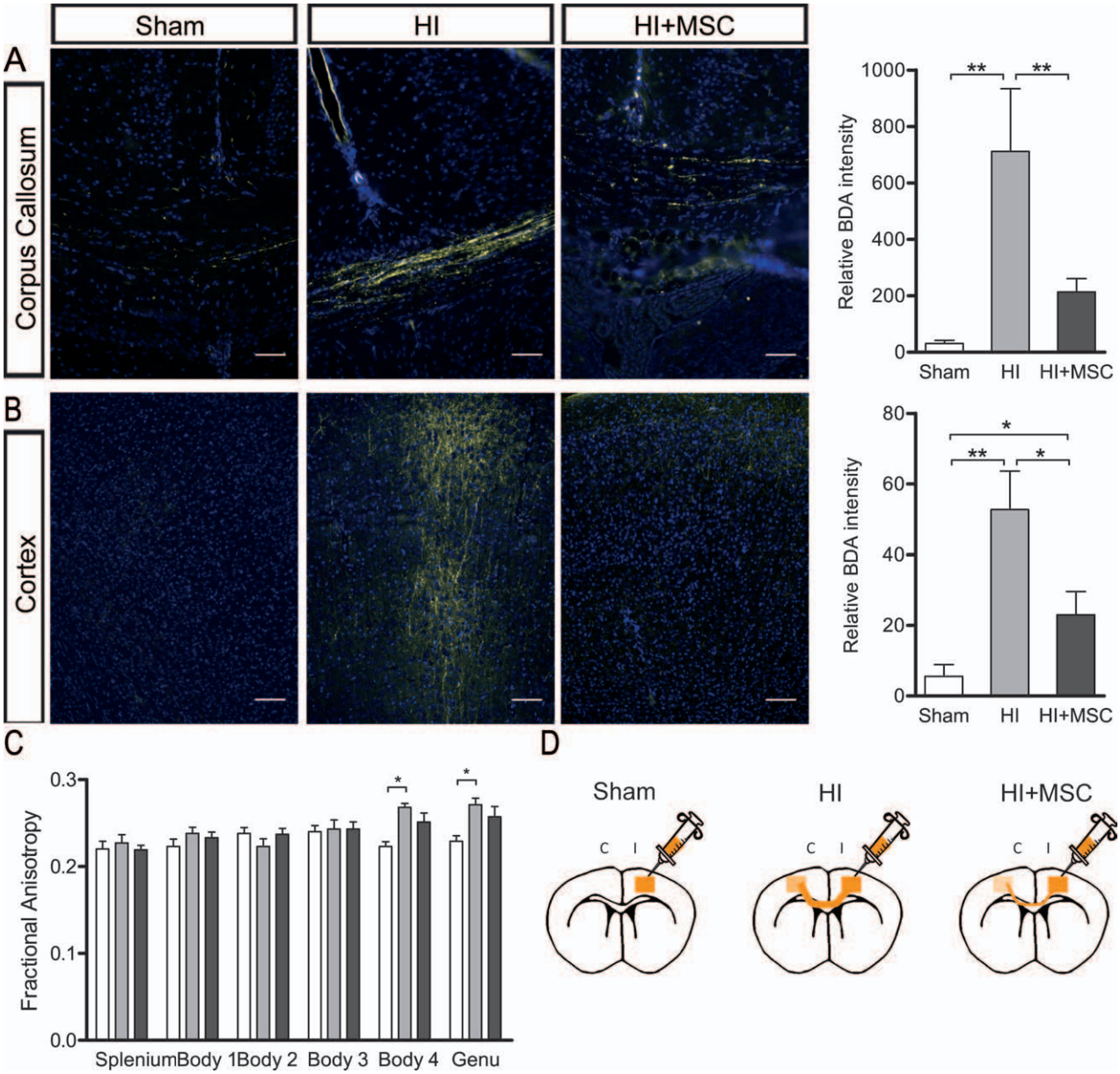

FIGURE 4: Connectivity between ipsilesional and contralesional motor cortices. At 21 days after hypoxia–ischemia (HI), biotinylated dextran amine (BDA) was injected into the ipsilesional motor cortex. Seven days later, we analyzed the intensity of BDA-positive staining (yellow) in (A) the corpus callosum as a measure of axons crossing the corpus callosum and in (B) the contralateral motor cortex as a measure of axonal projections to this area. BDA intensity in the corpus callosum and contralesional motor cortex was corrected for ipsilesional BDA intensity. Nuclei were stained in blue using DAPI. (C) Changes in fractional anisotropy in the contralesional cortex were measured using diffusion tensor imaging (DTI). (D) Schematic representation of BDA labeling pattern in sham operated mice and in HI and HI + mesenchymal stem cells (MSC) treated mice is shown. For BDA labeling analysis, n = 12 per group; n = 8 per group for DTI analysis. BDA labeling analysis and DTI analysis were performed in separate experimental groups. Data are expressed as mean ± standard error of the mean, *$p < 0.05$, **$p < 0.01$. Scale bar represents 50μm.

As a control, PRV-152-eGFP was injected into the right (unimpaired) forepaw (see Fig 5B). In all groups, eGFP labeling was found predominantly in the contralesional (left) motor cortex, and few eGFP-positive neurons were found in the ipsilesional motor cortex (see Fig 5E). Figure 5F depicts a schematic representation of PRV labeling in the brain.

Relation between Lesion Volume, Axonal Rewiring, and Motor Function

At 28 days after HI, there was an inverse relation between mean ipsilesional hemispheric volume and sensorimotor deficits, BDA intensity, and the number of RFP-positive neurons and thus contralesional rewiring (Fig 6A–C).

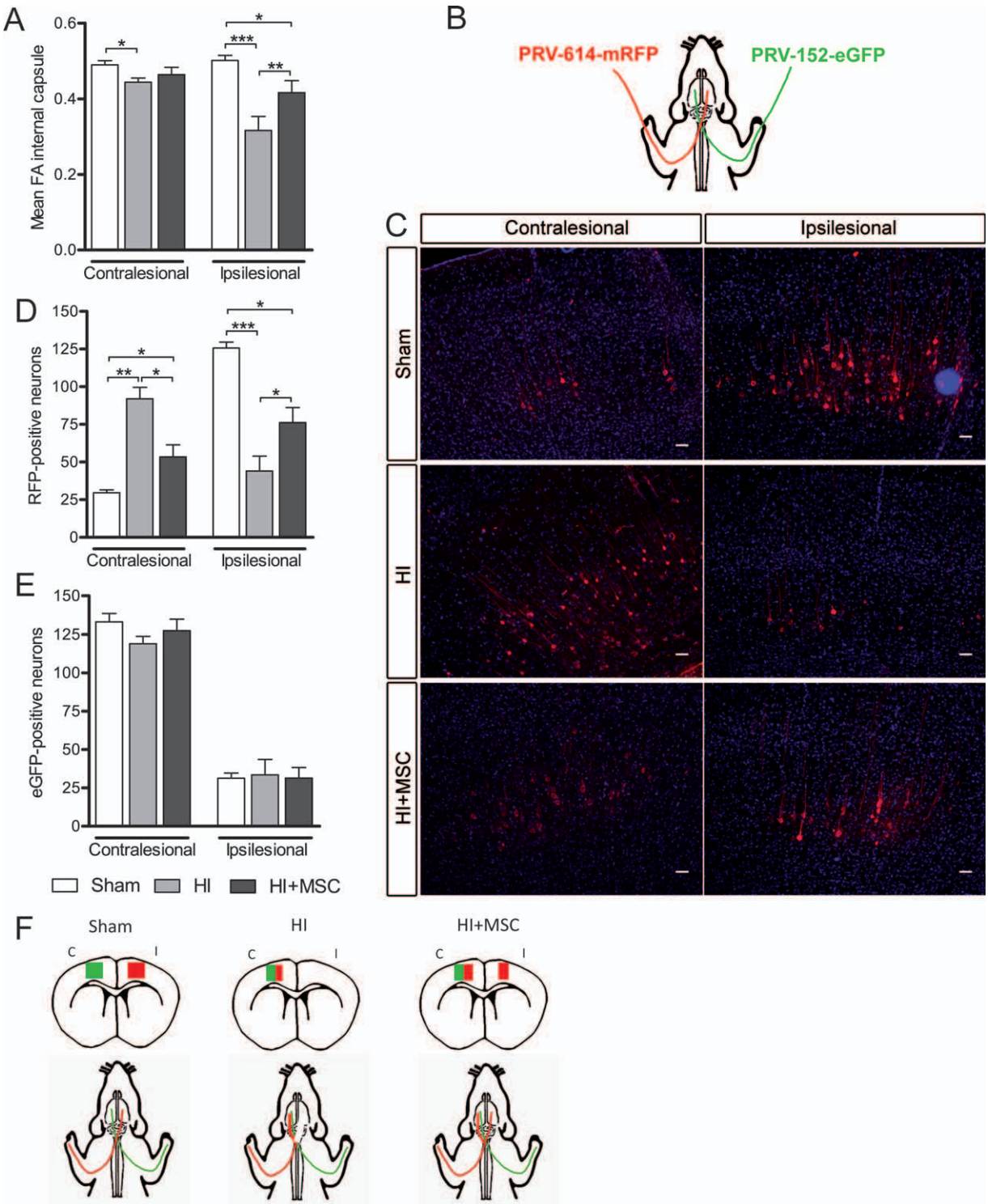

FIGURE 5: Functional connectivity between hypoxia–ischemia (HI)-impaired forepaw and contralesional motor cortex. (A) Changes in fractional anisotropy (FA) in the internal capsule were measured by diffusion tensor imaging (DTI) at day 28 after HI ± mesenchymal stem cell (MSC) treatment. (B) At 24 days after HI, PRV614-mRFP was injected into the left (impaired) forepaw, and PRV-152-eGFP was injected into the right (unimpaired) forepaw. (C) Representative photographs of PRV616-mRFP labeling in the motor cortex are shown. (D) PRV614-mRFP or (E) PRV-152-eGFP labeling was analyzed in the ipsilesional (right) and contralesional (left) motor cortex. For DTI analysis, n = 8 per group; n = 12 per group for pseudorabies virus (PRV) labeling analysis. DTI analysis and PRV labeling were performed in separate experimental groups. (F) Schematic representation of PRV labeling pattern in motor cortex is shown. Data are expressed as mean ± standard error of the mean, *$p < 0.05$, **$p < 0.01$.

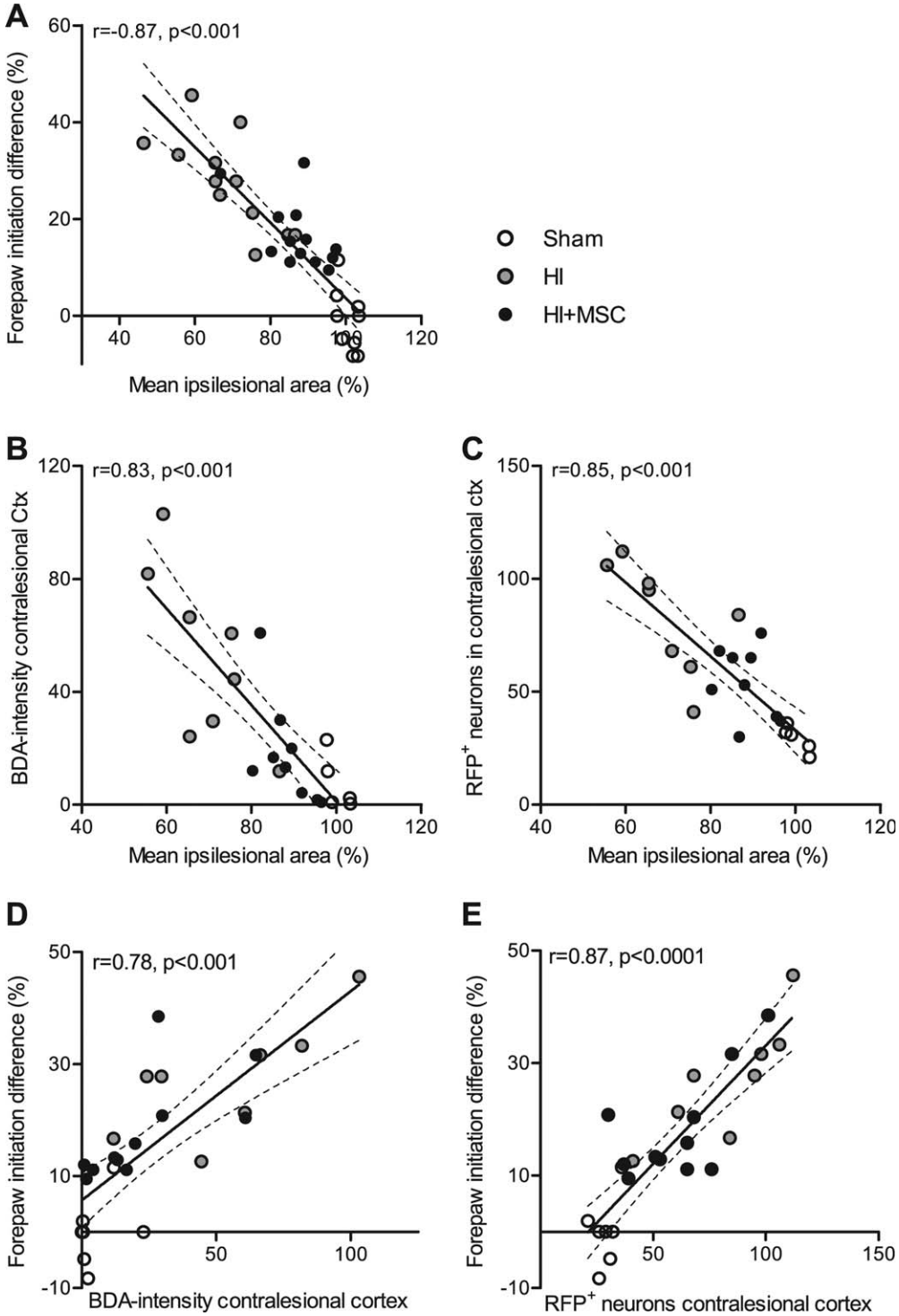

FIGURE 6: Relation between contralesional remodeling and functional outcome: relation between (A) mean ipsilesional area and forepaw initiation difference, (B) biotinylated dextran amine (BDA) intensity in the contralesional cortex (Ctx), and (C) red fluorescent protein (RFP)-positive neurons in the contralesional cortex. (D) Relation between forepaw initiation difference and BDA intensity in the contralesional cortex and (E) relation between forepaw initiation difference at 28 days after hypoxia–ischemia (HI) and RFP-positive neurons in the contralesional motor cortex are shown. Sham (white), n = 6; HI (gray), n = 9; HI + mesenchymal stem cell (MSC; black), n = 10.

Analysis of the relation between contralesional rewiring and sensorimotor deficits at 28 days after HI revealed a clear positive relation between contralesional BDA intensity and impaired sensorimotor function (see Fig 6D). The relation between contralesional rewiring and deteriorated sensorimotor function is further

strengthened by the positive relation between the number of RFP-positive neurons in the contralesional motor cortex and sensorimotor impairment (see Fig 6E).

Discussion

We provide for the first time an in-depth anatomical, microstructural, and microscopic characterization of the beneficial effects of MSC treatment after neonatal HI brain damage. Our novel data show that MSC treatment reduces HI-induced contralesional axonal rewiring, increases axonal connectivity in the ipsilesional hemisphere, and improves sensorimotor function. This axonal rewiring involves ultrastructural changes in CST architecture.

In the present study, MSC treatment reduced HI-induced changes in cortex and CC white matter architecture. However, DTI analysis in cortex and CC revealed a seemingly ambivalent relationship between FA values, $D_{//}$, $D_{\perp}$, and myelination. Although a large body of evidence supports the idea of a direct link between $D_{//}$ and axonal integrity and between $D_{\perp}$ and myelination, there is accumulating evidence that this link is not always so direct.[23,24] For example, both increased and reduced $D_{\perp}$ have been described in white matter damage due to neonatal HI.[25–27] In the present study, DTI analysis showed increased FA values and decreased $D_{\perp}$ after HI, which would indicate more myelination.[28,29] However, MBP intensity at the same levels was decreased in the same set of mice. Increased FA could point toward thicker myelin sheaths, decreased axonal diameter, and improved white matter organization.[30] Based on results showing that MBP-positive fibers have fewer arborizations, which increases their directionality (coherency), we propose that increased cortical FA after HI is due to altered white matter organization rather than to increased myelination.

In the CC, HI decreased FA values with decreased $D_{//}$, indicating loss of axonal integrity. Myelin plays a major role in maintaining axonal integrity.[31] Although primary axonal damage occurs after HI, failure of myelination may further contribute to reduced axonal integrity. Oligodendrocyte precursor cells are extremely vulnerable for HI; delaying the normal myelination process in HI mice results in white matter pathology also seen in the present study.[32,33] This delay in myelination could further contribute to decreased axonal integrity, which is reflected in the observed diffusivity values. MSC treatment induces maturation of oligodendrocytes to produce myelin in in vitro culture of neural stem cells.[34] Previously, we have also shown that upon MSC treatment more oligodendrocytes are formed, and myelin content in the ischemic hemisphere increases.[6,7] Stimulation of myelination by MSC treatment could be reflected by the observed normalization of diffusivity values.

A recent study showed that decreased MBP arborizations in the cortex of mice co-occurred with reduced rotarod performance.[35] Similarly, we show here that MSC treatment restored HI-induced subtle white matter abnormalities in the ipsilesional cortex concomitantly with reducing lateralizing motor deficits. In the CC, increased organization and myelination following MSC treatment may have major effects on decreasing lateralizing motor function. Mice with callosal agenesis or CC transsection exhibit greater laterality than controls.[36] Furthermore, in children with traumatic brain injury, decreased axonal organization in the midbody and genu of the CC is related to deteriorated fine motor speed and coordination.[37] Thus, reduced CC organization after HI could be an important underlying cause of the increased lateralizing motor deficits in HI mice, and reversely increased organization following MSC treatment could contribute to decreased lateralizing motor deficits.

The uninjured CST, which is the primary transmission route for voluntary forelimb movement, descends from the motor cortex via the IC toward the spinal cord.[38,39] In our previous study, we have shown that HI significantly reduces BDA labeling in the contralateral cervical spinal cord after BDA injection into the ipsilesional motor cortex.[6] Moreover, after MSC treatment BDA labeling in the contralateral spinal cord was significantly increased compared with HI mice. These findings indicate that MSC treatment restores HI-induced damage to the CST. Importantly, the results from the present study complement previously obtained results, as we show here that that following HI BDA labeling of the contralesional motor cortex occurs. This indicates rewiring of axons originating from the ipsilesional motor cortex toward the contralesional motor cortex, which is reduced by MSC treatment.

Using anterograde BDA tracing brings up the question of whether the observed results are really indicative of axonal rewiring or merely reflect BDA taking the path of least resistance (ie, enhanced axonal transport). Because rerouting of axons is dependent on axonal transport, BDA tracing alone does not allow a firm conclusion. However, in combination with retrograde PRV tracing, we conclude that contralesional axonal rewiring after HI and restoration due to MSC treatment do occur.

Disruption of normal CST routing after HI and restoration of CST routing after MSC treatment were also visible in the IC. DTI analysis showed that after HI fibers in both the ipsi- and contralesional IC are disorganized and following MSC treatment organization of fibers increased to sham level.

The extent of contralesional rewiring was related to the extent of lateralizing motor deficits.

The extent of BDA labeling both in the contralesional motor cortex and in the contralateral spinal cord are related to the extent of lateralizing motor deficits, indicating that normalization of CST routing by MSC treatment after neonatal HI is an important contributor of improved motor function. Although following MSC treatment BDA intensity in the contralesional motor cortex is decreased to sham level in some of the mice, their motor function is not completely restored. This indicates that normalization of contralesional rewiring alone is not sufficient to fully restore motor function and that other restorative processes in the ipsilesional hemisphere are likely required to normalize motor function completely. Our results show that lesion size is an important indicator of the extent of contralesional rewiring and lateralizing motor deficits. MSC treatment has been shown to stimulate several endogenous repair processes, like neurogenesis and angiogenesis, which are likely involved in the reduction of lesion size observed. Combined, our results indicate that several repair processes acting at the same time are needed to reach optimal repair of damage tissue and decrease lateralizing motor deficits.

Axonal rerouting can ensue through several processes, including sprouting of surviving neurons, neurite extension, synaptogenesis, and unmasking of existing functionally inactive networks.[40] Unmasking of dormant neural networks could be important, as new functional connections between motor cortex and peripheral targets like the forepaws after HI are rapidly needed. However, a more likely mechanism is axonal sprouting and synaptogenesis of surviving neurons.[41] Under normal circumstances, sprouting of axons into an environment containing myelin-derived inhibitors does not occur.[41] After HI, more ipsilesional motor cortex axons cross toward the contralesional cortex. This rerouting of axons could be due to decreased myelin content in the CC after HI. Vice versa, MSC treatment increases myelin content in the CC and may thereby reduce axons crossing the CC. Axonal sprouting, neurite extension, and synaptogenesis are tightly regulated by growth factors.[42] Previously, we have shown that MSC treatment induces ipsilesional expression of the growth cone molecule GAP43 and the synaptogenesis marker synaptophysin.[6] Moreover, MSC treatment after HI induces expression of *NRCAM*, *NGF*, *BDNF*, and *EFNB1*, factors known to play a role in neurite extension and outgrowth of axons.[43,44] Therefore, we propose that MSCs change the growth factor milieu in the brain to promote the reorganization of white matter tracts.

To the best of our knowledge, this study is the first to visualize remodeling of motor tracts in the brain after MSC treatment following neonatal HI brain injury. Moreover, we show for the first time that reduced contralesional remodeling after MSC treatment is positively related to motor performance. DTI analysis clearly showed that unilateral HI brain damage and subsequent MSC treatment induces changes throughout the brain. Anterograde and retrograde tracing complemented each other in showing functional contralesional rewiring of axons over the CC after HI, which was reduced after MSC treatment. Taking these observations together, we propose that MSC treatment is a promising therapeutic strategy to normalize ipsilesional motor tract routing and improved motor function. This is especially important because the devastating effects of neonatal encephalopathy often include motor problems.

Acknowledgment

This study was funded by the Wilhelmina Children's Hospital Research fund; European Union (LSHM-CT-2006-036534, NEOBRAIN; HEALTH-F2-2009-241778, NEUROBID); Swiss National Fund No. 31003A-112233; ELA Foundation; Biomedical Imaging Center of the University of Lausanne, University of Geneva, Vaud University Hospital Center, and Geneva University Hospitals; and Leenards and Jeantet foundations.

We thank Dr L. Enquist for PRV tracers and Dr H. Favoreel for PRV production.

Potential Conflicts of Interest

Nothing to report.

References

1. Armstrong-Wells J, Bernard TJ, Boada R, Manco-Johnson M. Neurocognitive outcomes following neonatal encephalopathy. Neuro-Rehabilitation 2010;26:27–33.
2. Ferriero DM. Neonatal brain injury. N Engl J Med 2004;351: 1985–1995.
3. Van Handel M, Swaab H, de Vries LS, Jongmans MJ. Long-term cognitive and behavioral consequences of neonatal encephalopathy following perinatal asphyxia: a review. Eur J Pediatr 2007; 166:645–654.
4. Thoresen M. Hypothermia after perinatal asphyxia: selection for treatment and cooling protocol. J Pediatr 2011;158(2 suppl):e45–e49.
5. Liu Z, Li Y, Zhang X et al. Contralesional axonal remodeling of the corticospinal system in adult rats after stroke and bone marrow stromal cell treatment. Stroke 2008;39:2571–2577.
6. van Velthoven CT, Kavelaars A, van Bel F, Heijnen CJ. Repeated mesenchymal stem cell treatment after neonatal hypoxia-ischemia has distinct effects on formation and maturation of new neurons and oligodendrocytes leading to restoration of damage, corticospinal motor tract activity, and sensorimotor function. J Neurosci 2010;30:9603–9611.

7. van Velthoven CT, Kavelaars A, van Bel F, Heijnen CJ. Mesenchymal stem cell treatment after neonatal hypoxic-ischemic brain injury improves behavioral outcome and induces neuronal and oligodendrocyte regeneration. Brain Behav Immun 2010;24:387–393.
8. Yasuhara T, Hara K, Maki M, et al. Intravenous grafts recapitulate the neurorestoration afforded by intracerebrally delivered multipotent adult progenitor cells in neonatal hypoxic-ischemic rats. J Cereb Blood Flow Metab 2008;28:1804–1810.
9. Lee JA, Kim BI, Jo CH, et al. Mesenchymal stem-cell transplantation for hypoxic-ischemic brain injury in neonatal rat model. Pediatr Res 2010;67:42–46.
10. Li Y, Chen J, Zhang CL, et al. Gliosis and brain remodeling after treatment of stroke in rats with marrow stromal cells. Glia 2005; 49:407–417.
11. Chen J, Li Y, Wang L, et al. Therapeutic benefit of intracerebral transplantation of bone marrow stromal cells after cerebral ischemia in rats. J Neurol Sci 2001;189:49–57.
12. Fromm C, Evarts EV. Pyramidal tract neurons in somatosensory cortex: central and peripheral inputs during voluntary movement. Brain Res 1982;238:186–191.
13. Hedtjarn M, Leverin AL, Eriksson K, et al. Interleukin-18 involvement in hypoxic-ischemic brain injury. J Neurosci 2002;22:5910–5919.
14. Zhu C, Wang X, Xu F, et al. The influence of age on apoptotic and other mechanisms of cell death after cerebral hypoxia-ischemia. Cell Death Differ 2005;12:162–176.
15. Clancy B, Finlay BL, Darlington RB, Anand KJ. Extrapolating brain development from experimental species to humans. Neurotoxicology 2007;28:931–937.
16. van der Kooij M, Ohl F, Arndt SS, et al. Mild neonatal hypoxia-ischemia induces long-term motor- and cognitive impairments in mice. Brain Behav Immun 2010;24:850–856.
17. Stejskal EO, Tanner JE. Spin diffusion measurements: spin echoes in the presence of a time-dependent field gradient. J Chem Phys 1965;42:288–292.
18. Basser PJ, Pierpaoli C. A simplified method to measure the diffusion tensor from seven MR images. Magn Reson Med 1998;39:928–934.
19. Neeman M, Freyer JP, Sillerud LO. A simple method for obtaining cross-term-free images for diffusion anisotropy studies in NMR microimaging. Magn Reson Med 1991;21:138–143.
20. Reiner A, Veenman CL, Medina L, et al. Pathway tracing using biotinylated dextran amines. J Neurosci Methods 2000;103:23–37.
21. Banfield BW, Kaufman JD, Randall JA, Pickard GE. Development of pseudorabies virus strains expressing red fluorescent proteins: new tools for multisynaptic labeling applications. J Virol 2003;77: 10106–10112.
22. Smith BN, Banfield BW, Smeraski CA, et al. Pseudorabies virus expressing enhanced green fluorescent protein: a tool for in vitro electrophysiological analysis of transsynaptically labeled neurons in identified central nervous system circuits. Proc Natl Acad Sci U S A 2000;97:9264–9269.
23. Wheeler-Kingshott CA, Cercignani M. About "axial" and "radial" diffusivities. Magn Reson Med 2009;61:1255–1260.
24. Field AS, Alexander AL, Wu YC, et al. Diffusion tensor eigenvector directional color imaging patterns in the evaluation of cerebral white matter tracts altered by tumor. J Magn Reson Imaging 2004;20:555–562.
25. Fatemi A, Wilson MA, Phillips AW, et al. In vivo magnetization transfer MRI shows dysmyelination in an ischemic mouse model of periventricular leukomalacia. J Cereb Blood Flow Metab 2011;31: 2009–2018.
26. Shereen A, Nemkul N, Yang D, et al. Ex vivo diffusion tensor imaging and neuropathological correlation in a murine model of hypoxia-ischemia-induced thrombotic stroke. J Cereb Blood Flow Metab 2011;31:1155–1169.
27. Chan KC, Khong PL, Lau HF, et al. Late measures of microstructural alterations in severe neonatal hypoxic-ischemic encephalopathy by MR diffusion tensor imaging. Int J Dev Neurosci 2009;27: 607–615.
28. Larvaron P, Boespflug-Tanguy O, Renou JP, Bonny JM. In vivo analysis of the post-natal development of normal mouse brain by DTI. NMR Biomed 2007;20:413–421.
29. Song SK, Yoshino J, Le TQ, et al. Demyelination increases radial diffusivity in corpus callosum of mouse brain. Neuroimage 2005; 26:132–140.
30. Barazany D, Basser PJ, Assaf Y. In vivo measurement of axon diameter distribution in the corpus callosum of rat brain. Brain 2009;132(pt 5):1210–1220.
31. Fancy SP, Chan JR, Baranzini SE, et al. Myelin regeneration: a recapitulation of development? Annu Rev Neurosci 2011;34: 21–43.
32. Levison SW, Rothstein RP, Romanko MJ, et al. Hypoxia/ischemia depletes the rat perinatal subventricular zone of oligodendrocyte progenitors and neural stem cells. Dev Neurosci 2001;23: 234–247.
33. Back SA, Han BH, Luo NL, et al. Selective vulnerability of late oligodendrocyte progenitors to hypoxia-ischemia. J Neurosci 2002; 22:455–463.
34. Zhang J, Li Y, Zhang ZG, et al. Bone marrow stromal cells increase oligodendrogenesis after stroke. J Cereb Blood Flow Metab 2009; 29:1166–1174.
35. Morello N, Bianchi FT, Marmiroli P, et al. A role for hemopexin in oligodendrocyte differentiation and myelin formation. PLoS One 2011;6:e20173.
36. Filgueiras CC, Manhaes AC. Increased lateralization in rotational side preference in male mice rendered acallosal by prenatal gamma irradiation. Behav Brain Res 2005;162:289–298.
37. Ewing-Cobbs L, Prasad MR, Swank P, et al. Arrested development and disrupted callosal microstructure following pediatric traumatic brain injury: relation to neurobehavioral outcomes. Neuroimage 2008;42:1305–1315.
38. Lama S, Qiao M, Kirton A, et al. Imaging corticospinal degeneration in neonatal rats with unilateral cerebral infarction. Exp Neurol 2011;228:192–199.
39. Liu Z, Zhang RL, Li Y, et al. Remodeling of the corticospinal innervation and spontaneous behavioral recovery after ischemic stroke in adult mice. Stroke 2009;40:2546–2551.
40. Carmichael ST. Themes and strategies for studying the biology of stroke recovery in the poststroke epoch. Stroke 2008;39: 1380–1388.
41. Benowitz LI, Carmichael ST. Promoting axonal rewiring to improve outcome after stroke Neurobiol Dis 2010;37:259–266.
42. Carmichael ST. Cellular and molecular mechanisms of neural repair after stroke: making waves. Ann Neurol 2006;59:735–742.
43. van Velthoven CT, Kavelaars A, van Bel F, Heijnen CJ. Mesenchymal stem cell transplantation changes the gene expression profile of the neonatal ischemic brain. Brain Behav Immun 2011;25: 1342–1348.
44. Qu R, Li Y, Gao Q, et al. Neurotrophic and growth factor gene expression profiling of mouse bone marrow stromal cells induced by ischemic brain extracts. Neuropathology 2007;27:355–363.